AGU PUBLICATIONS

JGR

Journal of Geophysical Research: Biogeosciences

RESEARCH ARTICLE
10.1002/2016JG003365

Key Points:
- Diffuse light increases over a narrow range of optically thin clouds ($\tau_c < 7$)
- The decrease in total light under optically thin cloud offsets increases in light-use efficiency
- Changes within $\tau_c < 7$ are unlikely to alter plant canopy CO_2 uptake

Supporting Information:
- Supporting Information S1

Correspondence to:
S. J. Cheng,
chengs@umich.edu

Citation:
Cheng, S. J., A. L. Steiner, D. Y. Hollinger, G. Bohrer, and K. J. Nadelhoffer (2016), Using satellite-derived optical thickness to assess the influence of clouds on terrestrial carbon uptake, *J. Geophys. Res. Biogeosci.*, *121*, 1747–1761, doi:10.1002/2016JG003365.

Received 2 FEB 2016
Accepted 14 JUN 2016
Accepted article online 15 JUN 2016
Published online 5 JUL 2016

Using satellite-derived optical thickness to assess the influence of clouds on terrestrial carbon uptake

S. J. Cheng[1], A. L. Steiner[2], D. Y. Hollinger[3], G. Bohrer[4], and K. J. Nadelhoffer[1]

[1]Department of Ecology and Evolutionary Biology, University of Michigan, Ann Arbor, Michigan, USA, [2]Department of Climate and Space Sciences and Engineering, University of Michigan, Ann Arbor, Michigan, USA, [3]Northern Research Station, USDA Forest Service, Durham, New Hampshire, USA, [4]Department of Civil, Environmental and Geodetic Engineering, The Ohio State University, Columbus, Ohio, USA

Abstract Clouds scatter direct solar radiation, generating diffuse radiation and altering the ratio of direct to diffuse light. If diffuse light increases plant canopy CO_2 uptake, clouds may indirectly influence climate by altering the terrestrial carbon cycle. However, past research primarily uses proxies or qualitative categories of clouds to connect the effect of diffuse light on CO_2 uptake to sky conditions. We mechanistically link and quantify effects of cloud optical thickness (τ_c) to surface light and plant canopy CO_2 uptake by comparing satellite retrievals of τ_c to ground-based measurements of diffuse and total photosynthetically active radiation (PAR; 400–700 nm) and gross primary production (GPP) in forests and croplands. Overall, total PAR decreased with τ_c, while diffuse PAR increased until an average τ_c of 6.8 and decreased with larger τ_c. When diffuse PAR increased with τ_c, 7–24% of variation in diffuse PAR was explained by τ_c. Light-use efficiency (LUE) in this range increased 0.001–0.002 per unit increase in τ_c. Although τ_c explained 10–20% of the variation in LUE, there was no significant relationship between τ_c and GPP ($p > 0.05$) when diffuse PAR increased. We conclude that diffuse PAR increases under a narrow range of optically thin clouds and the dominant effect of clouds is to reduce total plant-available PAR. This decrease in total PAR offsets the increase in LUE under increasing diffuse PAR, providing evidence that changes within this range of low cloud optical thickness are unlikely to alter the magnitude of terrestrial CO_2 fluxes.

1. Introduction

Clouds alter the Earth's energy balance in multiple ways, including through the greenhouse effect and changes in planetary albedo [*Arking*, 1991; *Stephens*, 2005]. Calculating the net effect of clouds on climate in Earth system models remains an important challenge [*Bony et al.*, 2015; *Boucher et al.*, 2013]. Much of the research addressing this has focused on understanding the radiative effects of clouds [*Andrews et al.*, 2012; *Lauer and Hamilton*, 2013]. However, clouds can also influence Earth's climate through the carbon cycle by changing the amount and type of light available for plants to use in photosynthesis [*Jenkins et al.*, 2007]. Similar to modeling clouds, difficulties in modeling the carbon cycle lead to projections of CO_2 fluxes into terrestrial ecosystems that carry large uncertainty. The most recent Earth system model intercomparison project estimates that terrestrial ecosystems can be either a source of or sink for carbon by 2100, with fluxes ranging from -6 to 9 Pg C yr^{-1} [*Friedlingstein et al.*, 2014]. One way to identify a potential source of uncertainty in land surface models, while also improving our understanding of how clouds impact climate, is to mechanistically link and quantify the effects of clouds on terrestrial CO_2 fluxes.

Clouds can influence the terrestrial carbon cycle by changing light availability in two ways. First, clouds can reduce the amount of light that reaches plant canopies by absorbing and reflecting solar radiation [*Cess et al.*, 1995; *Twomey*, 1991]. Second, cloud droplets and ice crystals interact with incoming solar radiation to produce scattered, diffuse light [*Davis and Marshak*, 2010; *Hansen*, 1971]. Regional climate model simulations demonstrate that model skill for estimating variability in summer temperatures improves when radiation is explicitly partitioned into direct and diffuse components, but only up to 3% [*Davin and Seneviratne*, 2012]. In addition, when more of the photosynthetically active radiation (PAR; 400–700 nm) above a light-saturated plant canopy is diffuse rather than direct, a greater percentage of incoming PAR is distributed to lower canopy leaves within the canopy [*Urban et al.*, 2012], which leads to an increase in canopy light-use efficiency (LUE) [*Gu et al.*, 2002; *Hollinger et al.*, 1994; *Knohl and Baldocchi*, 2008; *Niyogi et al.*, 2004; *Still et al.*, 2009]. Studies using modeled and measured diffuse PAR to predict ecosystem productivity infer that forest CO_2 uptake is greater under cloudy skies than under clear skies [*Law et al.*, 2002; *Rocha et al.*, 2004]. However, a

series of modeling studies collectively show that increases in LUE under diffuse light conditions may be too small to compensate for decreases in shortwave radiation on longer time scales [*Alton*, 2008; *Alton et al.*, 2005; *Knohl and Baldocchi*, 2008]. In contrast, a series of studies show that carbon uptake can be higher under diffuse light conditions, despite reductions in total PAR [*Gu et al.*, 1999; *Hollinger et al.*, 1994; *Mercado et al.*, 2009].

Although studies have examined the effect of diffuse light on terrestrial carbon processing, few have directly linked this relationship to clouds. Most studies have examined the assumption that clouds alter plant canopy uptake using proxies for cloud cover, rather than measurements of cloud properties [*Alton et al.*, 2005, 2007; *Gu et al.*, 1999; *Jenkins et al.*, 2007]. For example, cloud conditions have been inferred from the ratio of surface radiation to extraterrestrial radiation at the top of the atmosphere calculated from the solar constant and Earth-Sun geometry [*Liu and Jordan*, 1960]. Similarly, *Gu et al.* [1999] quantified cloudiness using the ratio of total radiation at the surface under a given sky condition to a modeled clear-sky radiation. However, these proxies are biased by the assumptions used to model and partition radiation [*Kanniah et al.*, 2012]. The use of observations of cloud cover would provide key empirical evidence of the impact of clouds on plant carbon uptake.

Of the studies using cloud observations, most use categorical descriptions of cloud cover (e.g., "cloud-free," "mixed," and "cloudy") [*Niyogi et al.*, 2004; *Oliphant et al.*, 2011]. This limits our ability to predict the effects of small changes in clouds that have been observed over the last few decades [*Free and Sun*, 2014; *Marchand*, 2013]. There is one study that used ground-based measurements of diffuse light and cloud measurements and found that surface diffuse light changes nonlinearly over a narrow range of cloud optical thickness (0 to 5), with a peak in diffuse light at a cloud optical thickness of 2 [*Min*, 2005]. However, this analysis was done at a single site, making it difficult to determine whether the effect of cloud optical thickness on carbon uptake can be applied to broader spatial scales. Another study used a satellite-retrieved measure of clouds (i.e., cloud fraction) from the International Satellite Cloud Climatology project (ISCCP) to show that satellite data over the Amazon can predict site-specific surface light conditions [*Butt et al.*, 2010]. However, this work did not connect cloud fraction to primary production or to areas beyond the region.

In this study, we use satellite-derived cloud optical thickness from Moderate Resolution Imaging Spectroradiometer (MODIS) instruments as a metric to mechanistically link and quantify the influence of clouds on surface diffuse light and canopy CO_2 uptake across multiple ecosystems. We use MODIS data because they are still collected, whereas ISCCP data are available only through 2009. We chose cloud optical thickness because it describes the cumulative depletion of light through a cloud [*Platnick et al.*, 2003]. It also combines the influence of cloud presence, physical thickness, and phase (i.e., liquid and solid) on the amount of surface radiation that is reflected, transmitted, and absorbed by the atmosphere [*Kikuchi et al.*, 2006; *Leontyeva and Stamnes*, 1994; *Platnick et al.*, 2003]. Cloud optical thickness (τ_c) is a dimensionless factor defined as

$$\tau_c = \int_0^d \beta(z)dz \tag{1}$$

where d is the height of the atmosphere and β is the cloud extinction coefficient, which is the sum of the scattering coefficient and absorption coefficient [*Mayer et al.*, 1998]. MODIS provides cloud τ_c at 1 km^2 resolution across the globe [*Platnick et al.*, 2003].

To identify whether there is an empirical link among clouds, diffuse PAR, and ecosystem carbon uptake, we combine MODIS τ_c values with ground observations of surface total and diffuse PAR and gross primary production (GPP) collected from a set of sites in the AmeriFlux network. We also use these data to identify if there is a signal of τ_c in GPP. Results from our study provide insights into how biosphere-atmosphere interactions influence the Earth's climate in two important ways. First, we evaluate the use of satellite-derived τ_c to determine the relationship between diffuse light and canopy CO_2 uptake identified in previous studies. This allows us to quantify the effects of clouds on carbon uptake and to identify how changes in clouds may alter fluxes of CO_2 into terrestrial ecosystems. Second, we quantify this effect at multiple sites of contrasting temperate zone ecosystem types (i.e., broadleaf forest, mixed forest, cropland). By linking and quantifying the relationships among τ_c, surface PAR, and GPP, we provide insight into how changes in clouds may impact climate through the carbon cycle by altering radiation regimes in terrestrial ecosystems.

2. Methods

2.1. Site Selection and AmeriFlux Data

To examine the relationships between τ_c, surface PAR, and GPP, we used ground-based observations provided through the AmeriFlux program (http://ameriflux.lbl.gov/). AmeriFlux is a network of flux and meteorological towers in the United States (U.S.) that measures fluxes of water vapor and CO_2 between the land surface and the atmosphere using the eddy covariance technique [*Baldocchi*, 2003], along with site-level soil, vegetation, radiation, and meteorological conditions. The online AmeriFlux data we used are standardized, reviewed, and quality controlled.

For the first part of our analysis, we analyzed the relationships between τ_c and both surface total and diffuse PAR. We chose AmeriFlux sites that are minimally managed, temperate ecosystems that have at least 3 years of CO_2 flux, total PAR, diffuse PAR, and MODIS data available (2000 to present) [*Platnick et al.*, 2003]. Eight sites (Table 1) met these criteria. For these sites, we used Level 2, with-gap (processed and quality controlled) diffuse PAR data from May through September available at 30 min or 1 h resolution to capture the primary Northern Hemisphere growing season. For Howland Forest, we included April data when this month was calculated as part of the site's peak growing season (see below for details).

Diffuse PAR was measured at Sherman Island with a custom-designed rotating shadow band radiometer. As the shadow band rotates around the photodiode in the radiometer, measurements of global (i.e., direct and diffuse) and diffuse light are recorded when the sensor is fully shaded and covered [*Michalsky et al.*, 1988]. At the remaining sites, diffuse PAR was measured with a model BF2, BF3, or BF5 sensor (Delta-T Devices, Ltd., Cambridge, UK).

For the second part of the analysis, we analyzed the relationship between τ_c and GPP, which is directly linked with light and, unlike net ecosystem exchange (NEE), does not include respiration. Of the eight sites with diffuse PAR measurements, only four had Level 2 NEE and with-gap GPP data. These sites represent mixed forest (Howland Forest), deciduous broadleaf forest (Morgan Monroe and the University of Michigan Biological Station; UMBS), and cropland (Mead Irrigated Maize). At these sites, ecosystem respiration is modeled from nighttime measurements and then subtracted from observed NEE to calculate GPP.

2.2. MODIS Cloud Optical Thickness (τ_c)

MODIS τ_c measurements are globally available at 1 km^2 resolution [*Platnick et al.*, 2003]. The MODIS instrument is a 36-band spectroradiometer measuring radiation between 0.415 and 14.235 μm from 705 km above Earth's surface aboard two satellites, Terra and Aqua [*Platnick et al.*, 2003]. Terra moves in a descending orbit and crosses the equator at approximately 10:30 local time, and Aqua moves in an ascending orbit with an overpass at the equator of approximately 13:30 local time [*Qu*, 2006]. MODIS has a 2330 km swath width, which leads to global coverage approximately every 2 days [*King et al.*, 2003]. Level 2 MODIS data are stored in 5 min data granules typically containing 2030 along-track pixels [*Baum and Platnick*, 2006].

Daytime τ_c values over land are retrieved using look-up tables to find the combinations of τ_c and cloud droplet effective radius values that best match solar reflectance measurements from one visible band (0.645 μm) and multiple near-infrared (1.6, 2.13, and 3.75 μm) bands [*Platnick et al.*, 2003; *King et al.*, 1997]. Calculations are made assuming plane-parallel, homogenous clouds over a black surface with no atmosphere and use separate libraries for ice and liquid water clouds [*Baum and Platnick*, 2006]. Additional algorithms correct for the effects of surface albedo and atmospheric transmittance on reflectance measurements, such as Rayleigh scattering and trace gas and water vapor absorption [*Platnick et al.*, 2003; *King et al.*, 1997].

An uncertainty value is also calculated for each τ_c that accounts for several types of errors. These include errors in the models and libraries used in the retrieval, changes to instrument calibration, and changes in the composition of the atmosphere above the cloud, such as aerosols and water vapor [*King et al.*, 1997]. Uncertainties in the retrieval process, such as for cloud cover, phase, particle size and shape, and homogeneity, bias estimates of τ_c, particularly for thin and thick clouds [*Zeng et al.*, 2012]. To minimize the effect of bias from retrieval uncertainties in our study, we limit our analysis to values of τ_c with uncertainty $<25\%$.

We used daytime, Level 2 Terra and Aqua cloud products (MOD06_L2, MYD06_L2) from Collection 5.1 from NASA's Level 1 and Atmosphere Archive and Distribution System (https://ladsweb.nascom.nasa.gov/index.html). The algorithms in this collection retrieve τ_c for pixels with a cloud mask designation of cloudy or probably cloudy [*King et al.*, 2013]. However, they do not process pixels that are identified as partly cloudy [*King*

Journal of Geophysical Research: Biogeosciences

10.1002/2016JG003365

Table 1. AmeriFlux Site Information and Ecosystem Characteristics

Site (SiteID)	Lat, Lon (°N, °W)	Years of Diffuse PAR Data	Canopy Height (m)	Vegetation Community	Management	LAI (m^2 m^{-2})	Average Cumulative May–Sep Precipitation (mm)	GPP	Average Peak Growing Season Start Date (DOY)	Growing Season Length in Days (Min, Max)
Howland Forest (US-Ho1)	45.204, 68.740	2006–2008	20[a]	Red spruce (*Picea rubens*) and Eastern hemlock (*Tsuga canadensis*) with balsam fir (*Abies balsamea*), white pine (*Pinus strobus*), white cedar (*Thuja occidentalis*), red maple (*Acer rubrum*), and paper birch (*Betula papyrifera*)[b]	None	~6[a]	358 (includes April)	Yes	141	106, 141
Mead (US-Ne1)	41.165, 96.476	2001–2012	2.9[c]	Maize (*Zea mays*)[d]	Center-pivot irrigation[d]	5.7[c]	630	Yes	184	31, 56
Morgan Monroe (US-MMS)	39.323, 86.413	2006–2013	27[e]	Sugar maple (*A. saccharum*), tulip poplar (*Liriodendron tulipifera*), sassafras (*Sassafras albidum*), white oak (*Quercus alba*), and black oak (*Q. nigra*)[e]	None	5[f]	495	Yes	142	41, 121
UMBS (US-UMB)	45.559, 84.713	2007–2012	22[g]	Bigtooth aspen (*Populus grandidentata*), red oak (*Q. rubra*), red maple (*A. rubrum*), and white pine (*P. strobus*) with trembling aspen (*P. tremuloides*), white birch (*B. papyrifera*), sugar maple (*A. saccharum*), red pine (*P. resinosa*), and American beech (*Fagus grandifolia*)[g]	None	~3.5[g]	355	Yes	164	51, 106
Bartlett (US-Bar)	44.064, 71.288	2004–2011	22[h]	American beech (*F. grandifolia*), sugar maple (*A. saccharum*), yellow birch (*Betula alleghaniensis*) with red maple (*A. rubrum*), paper birch (*B. papyrifera*), eastern hemlock (*T. canadensis*), eastern white pine (*P. strobus*), and red spruce (*Picea rubens*)[h]	None	3.6[h]	589	No	--	–
Flagstaff (US-Fuf)	35.089, 111.762	2006–2010	18[i]	*Pinus ponderosa* (Ponderosa pine)[i]	None	2.3[i]	301	No	--	–
Sherman Island (US-Snd)	38.037, 121.753	2010–2013	--	Grasses, including pepperweed (*Lepidium latifolium*) and mouse barley (*Hordeum murinum L.*)[j]	None	0.68-0.81[j]	13	No	--	–
Vaira Ranch (US-Var)	38.406, 120.950	2006–2013	0.55[k]	Grasses, including purple false brome (*Brachypodium distachyon L.*), smooth cat's ear (*Hypochaeris glabra L.*), lesser trefoil (*Trifolium dubium Sibth.*) rose clover (*Trifolium hirtum All.*), twinning snakelily (*Dichelostemma volubile A.*), and Big Heron bill (*Erodium botrys Cav*)[k]	Grazed[k]	<2[l]	35	No	--	–

[a] *Scott et al.* [2004].
[b] *Hollinger et al.* [2004].
[c] Personal communication with site investigator.
[d] *Suyker and Verma* [2008].
[e] *Dragoni et al.* [2011].
[f] *Oliphant et al.* [2011].
[g] *Gough et al.* [2013].
[h] *Jenkins et al.* [2007].
[i] *Dore et al.* [2012].
[j] *Ma et al.* [2012].
[k] *Xu and Baldocchi* [2004].
[l] *Miller et al.* [2007].

et al., 2013], which are included in the most recent collection [*Pincus et al.*, 2012]. Our results therefore reflect the effect of overcast skies within a $3 \times 3\ km^2$ area on surface light and GPP. Latitude and longitude coordinates from MODIS Level 1 Geolocation product (MOD03) were used to find the closest pixel within 0.01° of each AmeriFlux site. We compared the influence of τ_c on diffuse PAR using τ_c at two spatial resolutions: (1) τ_c from the $1 \times 1\ km^2$ pixel that includes the AmeriFlux site and (2) the mean τ_c from nine pixels covering a $3 \times 3\ km^2$ area with the AmeriFlux site in the center pixel of the pixel array. We did not apply filters to the pixels surrounding the center pixel. Calculations of mean τ_c therefore include pixels surrounding the center pixel with missing data and any uncertainty level. At $1 \times 1\ km^2$ resolution, all sites showed a similar nonlinear response of diffuse PAR to τ_c, except for Flagstaff (Figure S1 in the supporting information). However, when we used the average τ_c from a $3 \times 3\ km^2$ area, the response at Flagstaff matched the other sites. The larger spatial resolution may better explain the response of diffuse PAR to τ_c because a broader spatial area captures the spatial heterogeneity that may affect the half-hour or hourly ground-based diffuse PAR measurements. For the remainder of this paper, τ_c refers to the average τ_c from a $3 \times 3\ km^2$ area with the site at the center.

2.3. Peak Growing Season Calculations

For each site, we analyze GPP data for the most photosynthetically active time of year. To define this time period, we use changes in NEE to identify phenological changes in the plant canopy [*Garrity et al.*, 2011]. We calculate 5 day averages from daytime NEE (AmeriFlux Level 2 gap-filled data when available, otherwise Level 2 with-gap data) and define the first day of the peak growing season when the 5 day NEE average is within 90% of the year's fourth highest 5 day NEE average. We used the fourth-highest NEE average to account for extreme values due to anomalous weather. Next, we define the end of the peak growing season as the last day when the 5 day NEE average is within 75% of the year's fourth-highest NEE average. We use different cutoffs for the beginning and end of the season because phenological changes in the canopy are quicker in the beginning of the season (e.g., leaf out) than they are at the end (e.g., senescence). Although this approach cannot detect the exact beginning and end of the peak growing season, it provides a uniform method to define the period of time during which plants are at full seasonal growth and activity across our sites. In addition, only using data from the peak growing season allows us to quantify the maximum effect that clouds and diffuse light have on GPP.

2.4. Data Analysis

After obtaining τ_c values retrieved from MODIS, we matched each τ_c timestamp to the closest AmeriFlux tower time. The τ_c retrievals at our sites occurred during midday (10:00–15:00) and fell within a small range of zenith angles (16–30°). We excluded data points with missing vapor pressure deficit (VPD), air temperature, diffuse PAR, and total PAR and only used total PAR values $>20\ \mu mol\ m^{-2}\ s^{-1}$, assuming that lower radiation levels indicate sensor errors or marginal weather conditions (e.g., rain events). Under clear skies, aerosols, ozone, and humidity also affect the partitioning of direct solar radiation into diffuse light [*Bird and Riordan*, 1986]. We do not specifically include the effect of aerosols on surface PAR or GPP in our analysis because (1) aerosols have a relatively low optical depth compared to clouds (usually $\tau < 1.0$); (2) satellite-derived aerosol optical depth is not retrieved when clouds are present, which is the focus of this study; and (3) remote sites such as ours generally have low aerosol optical depths relative to areas closer to anthropogenic activity [*Steiner et al.*, 2013].

Because clouds both transmit and absorb diffuse light, we expected diffuse light to increase and then decrease with τ_c. To identify the point of τ_c where the relationship between these two variables first changed from positive to negative, we used a smoothing spline function [*R Core Team*, 2014]. This identifies the range of τ_c when clouds increase diffuse light and are most likely to increase GPP. The region where diffuse PAR increases with τ_c met the statistical assumptions of linear regression analysis, which we used to quantify the relationship between cloud τ_c and surface diffuse light. We analyzed the relationship between τ_c and diffuse PAR by month and found no large variation across the season. We also used a spline function to assess the response of total PAR across the entire range of τ_c. For two of the sites (Flagstaff and Howland), the residuals from the linear models between total PAR and τ_c while diffuse PAR increased did not pass the Shapiro-Wilk test or visual inspection for normality. However, we kept these data untransformed to display the information in a consistent format as the other sites and for the diffuse PAR data.

We also used linear regression analysis to examine the relationship between τ_c and GPP across the entire range of available τ_c data, which met statistical assumptions of this analysis method. The residuals from linear

models between LUE and τ_c below the maximum amount of diffuse PAR were not normal at all sites, but applying a log transformation to LUE produced normal residuals. Because the difference in R^2 did not increase more than 0.04, we report untransformed LUE data in the following analysis. Regressions between τ_c while diffuse PAR increased and transformed LUE are shown in Figure S2. For LUE data above the τ_c value associated with maximum diffuse PAR, all but one site met the assumptions for linear regression. We kept these data untransformed to keep all data in a consistent format.

3. Results and Discussion

3.1. τ_c and Diffuse PAR

Our analysis of τ_c and surface light above plant canopies at eight AmeriFlux sites shows a nonlinear relationship between τ_c and diffuse PAR (Figure 1). Across all sites, diffuse PAR increases with τ_c until an average value of 6.8, above which diffuse PAR decreases. There is some site-level variation in this value of τ_c, ranging from 5.2 at Flagstaff to 9.7 at Sherman Island (Figure 1). To our knowledge, only one study has used measurements of τ_c to examine cloud effects on surface diffuse PAR [*Min*, 2005]. That study used measurements from a multifilter rotating shadowband radiometer at one location (Harvard Forest) during one growing season to demonstrate that diffuse PAR increases up to $\tau_c = 2$ and decreases thereafter. Using new data, including satellite retrievals of τ_c and direct measurements of diffuse PAR from tower-mounted sensors, we expand this analysis across both space and time. We find that the response of diffuse PAR to τ_c is consistent across sites, yet diffuse PAR peaks at greater τ_c values than previously reported by *Min* [2005]. Our estimated values for the τ_c where diffuse PAR reaches its maximum, may be larger because we used data with solar zenith angles between 16 and 30°, whereas *Min* [2005] used data from more zenith angles.

Quantifying the range across which diffuse PAR and τ_c increase together is important for understanding canopy GPP fluxes because total PAR decreases across the entire range of τ_c (Figure 2). Below the τ_c value at which diffuse PAR peaks, we found significant positive relationships between τ_c and diffuse PAR at all sites ($p < 0.05$; Figure 3) except Flagstaff. The variation in diffuse PAR that is explained by τ_c at these sites ranges from 7 to 24% (Figure 3). The increase in diffuse PAR across this range of optically thin clouds ranged from 30 μmol m^{-2} s^{-1} per unit τ_c at Sherman Island to 71 μmol m^{-2} s^{-1} per unit τ_c at Vaira Ranch. These results illustrate the variability in light extinction in the atmosphere that occurs across sites. In addition, below a τ_c of 10, changes in total and diffuse PAR indicate that total PAR becomes increasingly dominated by diffuse PAR as τ_c increases (Figure 3). Thus, increases in τ_c above 10 predominately serve to reduce diffuse PAR above plant canopies.

Limitations in the cloud retrieval methods may explain some of the remaining variation in the relationship between τ_c and diffuse PAR. For example, satellite retrieval methods and ground-based sensors cannot entirely capture the impact of vertical and horizontal cloud heterogeneity on surface light. Cloud particle size, phase, and shape alter scattering properties of clouds (e.g., single scattering albedo) [*Chou et al.*, 1998; *King*, 1987; *Macke et al.*, 1998], which could cause clouds with the same τ_c to produce different amounts of diffuse light. The effect of cloud heterogeneity can also cause additional biases in satellite retrievals of τ_c by violating the MODIS algorithm assumption that clouds are homogenous [*Dim et al.*, 2007; *Zeng et al.*, 2012]. This has been seen in cloud resolving simulations and radiation schemes that demonstrate that the parameterization of cloud overlap influences model estimates of surface radiation [*Barker et al.*, 1999; *Shonk et al.*, 2010]. In addition, inaccurate algorithm selection of phase and cloud-scattering properties for inhomogeneous skies can bias retrievals of τ_c [*Koren et al.*, 2008; *Pincus et al.*, 2012; *Várnai and Marshak*, 2002]. Our use of the nine-pixel average of τ_c allows us to capture some of the horizontal inhomogeneity in clouds that would not be possible if we only used the τ_c from one pixel alone. The average minimum and maximum standard deviation of τ_c over a 3×3 km^2 area ranged from 0.11 to 4.36 (Table 2). This suggests the potential importance of spatial variability in cloud conditions (Table 2).

Some of the unexplained variation in the relationship between τ_c and diffuse PAR may also result from differences in the temporal and spatial resolutions between MODIS retrievals and AmeriFlux data. MODIS retrievals are near instantaneous (5 min per granule) and cover a 1 km^2 area, while AmeriFlux data are averaged at 30 min or 1 h and are made with point sensors. As a result, changes in cloud conditions included in the MODIS retrievals may not be entirely captured by ground-based PAR sensors, and vice versa. In addition,

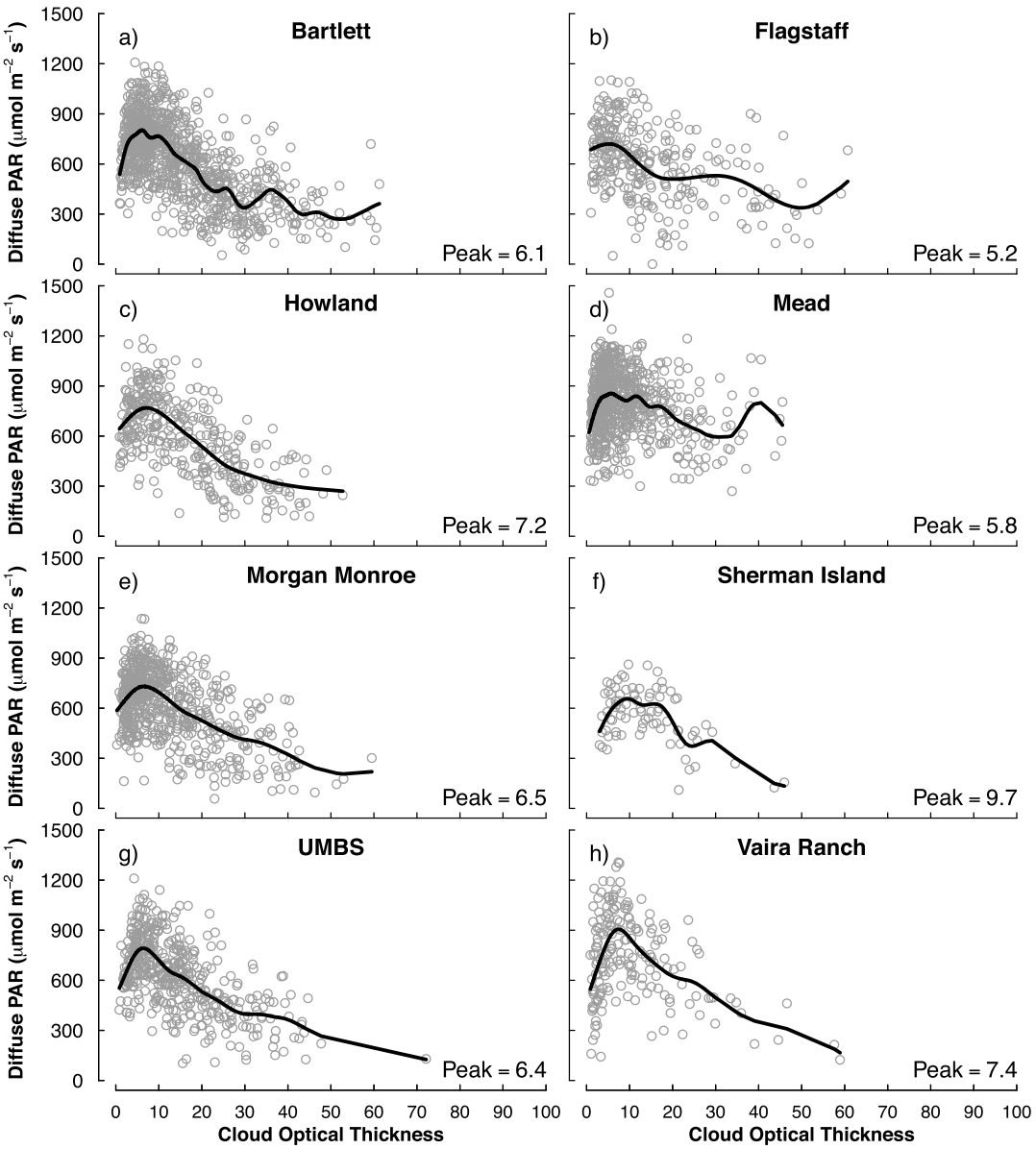

Figure 1. The response of AmeriFlux-tower measured diffuse photosynthetically active radiation (PAR; μmol m^{-2} s^{-1}) to 3 × 3 km^2 average cloud optical thickness (τ_c; unitless) with uncertainty <25% retrieved from MODIS. "Peak" refers to the highest value of τ_c associated with an increase in diffuse PAR. Data points include measurements from May through September from years with available data (see Table 1). For Howland Forest, April data are included when this month is calculated as part of the site's peak growing season. The plotted lines represent the general relationship between diffuse PAR and τ_c as estimated by a smoothing spline function.

variation across sites could result from calibration and measurement errors in ground-based PAR sensors. Despite these limitations, we still detect a signal of cloud optical thickness in surface diffuse PAR measurements.

3.2. τ_c and Light-Use Efficiency

For the four AmeriFlux sites with GPP measurements, we examined the relationship between τ_c and GPP per unit of total PAR, which describes ecosystem-level LUE. To capture any negative or positive effects of clouds on ecosystem carbon processing, we analyzed how LUE changes with τ_c under two separate regimes—first, when diffuse PAR increases with τ_c and second, when diffuse PAR decreases with τ_c. The separation between these two regimes is shown in Figure 4 with a vertical dashed line for each site, where diffuse PAR increases to the left of the line and diffuse PAR decreases to the right of the line. The calculations of τ_c where the maximum diffuse PAR occurs at each site, are shown in Figure 1 and explained in section 3.1.

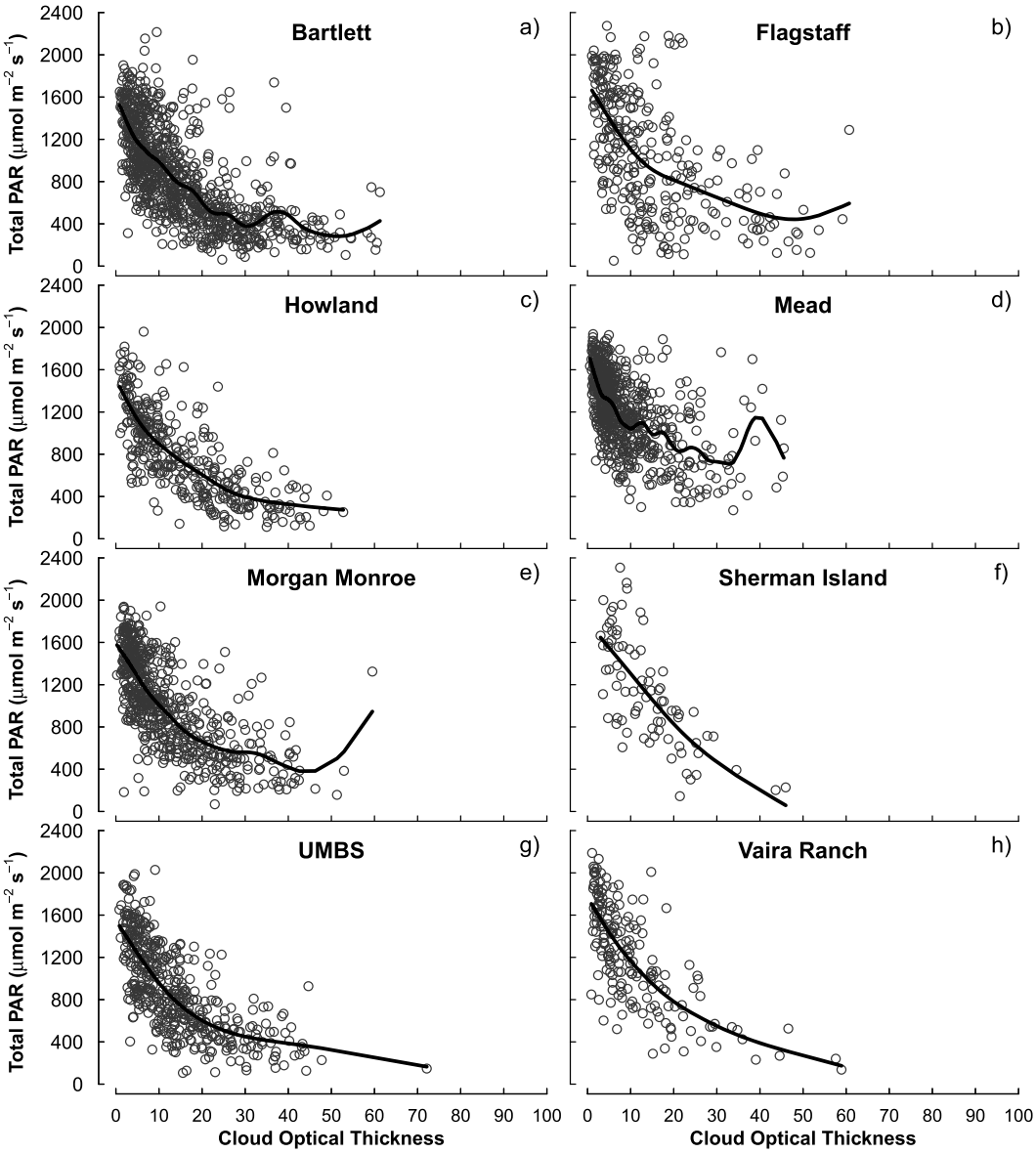

Figure 2. The response of AmeriFlux-tower measured total photosynthetically active radiation (PAR; μmol m^{-2} s^{-1}) to 3×3 km^2 average cloud optical thickness (τ_c; unitless) with uncertainty $< 25\%$ retrieved from MODIS. Data points include measurements from May through September from years with available data (see Table 1). For Howland Forest, April data are included when this month is calculated as part of the site's peak growing season. The plotted lines represent the general relationship between total PAR and τ_c as estimated by a smoothing spline function.

Interpreting the response of LUE to changes in τ_c and diffuse PAR is complicated by the overall decrease in total PAR that occurs as clouds become optically thick. Because photosynthesis rates increase and then saturate with PAR, LUE generally increases when total light availability decreases [*Medlyn*, 1998; *Turner et al.*, 2003]. Thus, it is expected that LUE would increase as clouds become more optically thick. Below, we discuss trends in LUE when PAR decreases but becomes more diffuse (low τ_c), as well as when both total and diffuse PAR decrease (higher τ_c).

Across the range of τ_c when diffuse PAR increases, LUE increases with τ_c ($p < 0.01$; Figure 4). The increases in LUE from the smallest to largest τ_c shown to the left of the vertical dashed lines in Figure 4 are 71% at Howland, 22% at Mead, 62% at Morgan Monroe, and 60% at UMBS. Although these percent increases are large in the forests, the increase in LUE across this range of τ_c was 0.001–0.002 per unit increase in τ_c. Our

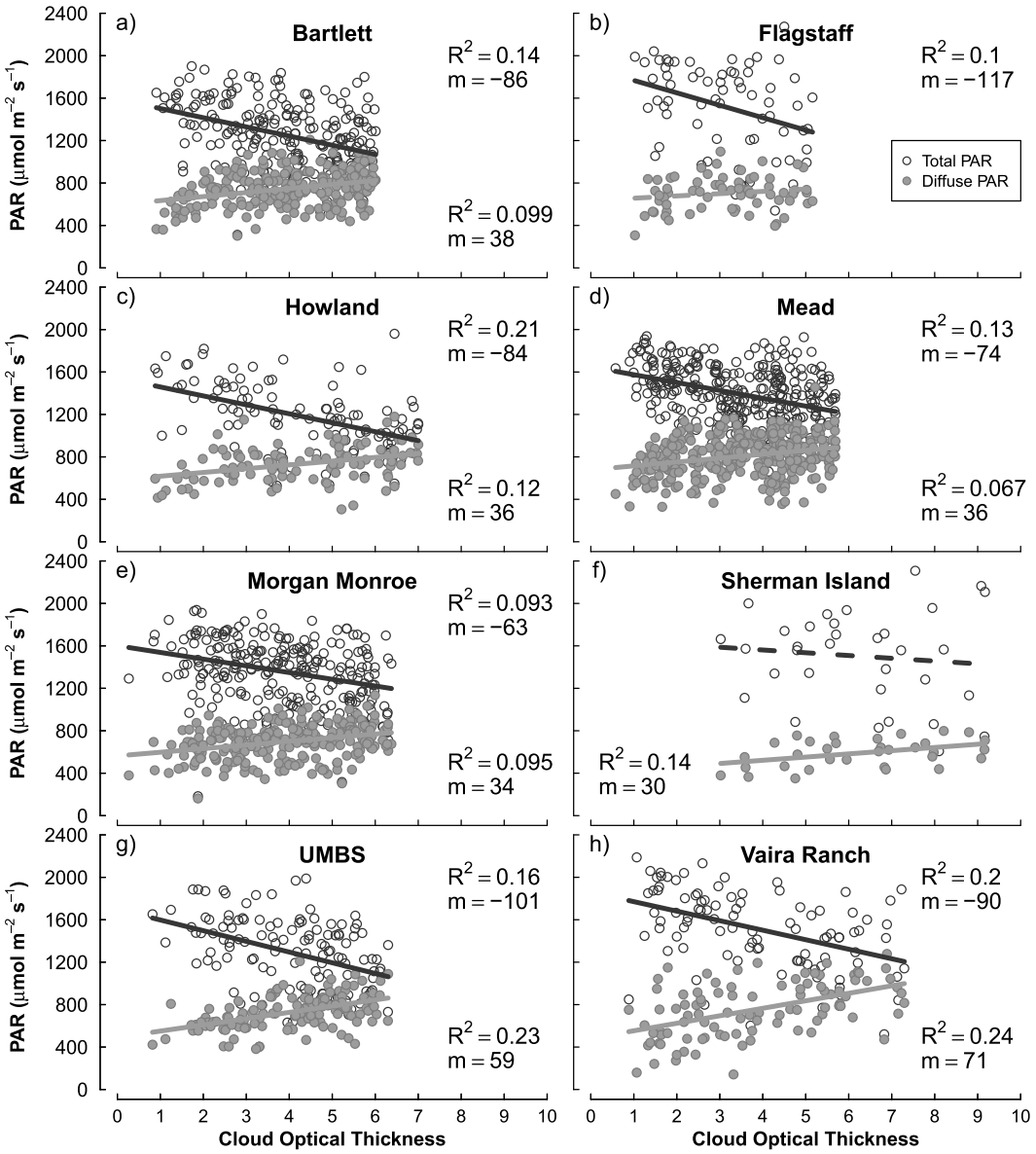

Figure 3. Relationship between diffuse and total photosynthetically active radiation (PAR; $\mu mol\, m^{-2}\, s^{-1}$) measured at AmeriFlux sites and $3 \times 3\ km^2$ average cloud optical thickness (τ_c; unitless) retrieved from MODIS. Data points include measurements from May through September from years with available data and for τ_c values lower than the peak of the diffuse PAR-τ_c curve (values listed in Figure 1). For Howland, April data are included when they are calculated as part of the site's peak growing season. R^2 and slopes (m) are listed for significant linear relationships with a $p < 0.05$.

results are consistent with the range of increases in LUE found on cloudy days compared to sunny days in a Sitka spruce forest [*Dengel and Grace*, 2010] and with the 39% increase in LUE found in a deciduous temperate forest under thin clouds compared to skies with aerosols [*Min*, 2005]. However, *Alton et al.* [2007] reported smaller increases in LUE, ranging from 6 to 18% in a boreal needleleaf forest and 15 to 28% in a temperate broadleaf forest depending on time of day. These rates may differ from ours because they defined LUE as the increase in GPP when diffuse fraction moves from below 0.5 to above 0.5, whereas we calculated LUE across a broader range of diffuse fraction for τ_c below the maximum amount of diffuse PAR for each site.

Both the strength of the response between LUE and τ_c as well as the degree of variation around this relationship varied between sites. Site-specific increases in LUE may be a result of the way plant canopy structure influences the distribution of light within the canopy [*Cheng et al.*, 2015]. The distribution of leaf area and the location of gaps

Table 2. Standard Deviation (SD) of τ_c for Retrievals Within a $3 \times 3\ km^2$ Area of Each AmeriFlux Site[a]

Site	Mean SD of τ_c	Minimum SD of τ_c	Maximum SD of τ_c
Flagstaff	0.82	0.08	3.29
Sherman Island	1.73	0.48	3.79
UMBS	1.29	0.14	4.78
Bartlett	1.05	0.04	4.45
Mead	0.99	0.07	5.38
Howland	0.91	0.03	3.89
Vaira Ranch	0.92	0.00	4.21
Morgan Monroe	0.82	0.06	5.05

[a]Data include points with a $3 \times 3\ km^2$ τ_c that is below the τ_c where diffuse PAR peaks and that occur during the sites' peak growing seasons.

in a plant canopy control light extinction and thus, how efficiently leaves absorb incoming PAR. Model simulations and field measurements demonstrate that different parts of the forest canopy contribute to total canopy photosynthesis when diffuse light changes [*Knohl and Baldocchi*, 2008; *Urban et al.*, 2012]. Thus, canopy characteristics can interact with above-canopy meteorological conditions to create canopy microclimates that change the effect of clouds and diffuse PAR on ecosystem productivity.

Finally, across the range of τ_c where diffuse PAR decreases, LUE increases with τ_c, as expected with declines in PAR (Figure 4 data to the right of the vertical dashed lines). In addition, LUE may also increase with τ_c because clouds can improve water and temperature conditions for photosynthesis [*Urban et al.*, 2007]. Importantly, we found that the rate of increase in LUE under optically thick clouds is 1 order of magnitude smaller than

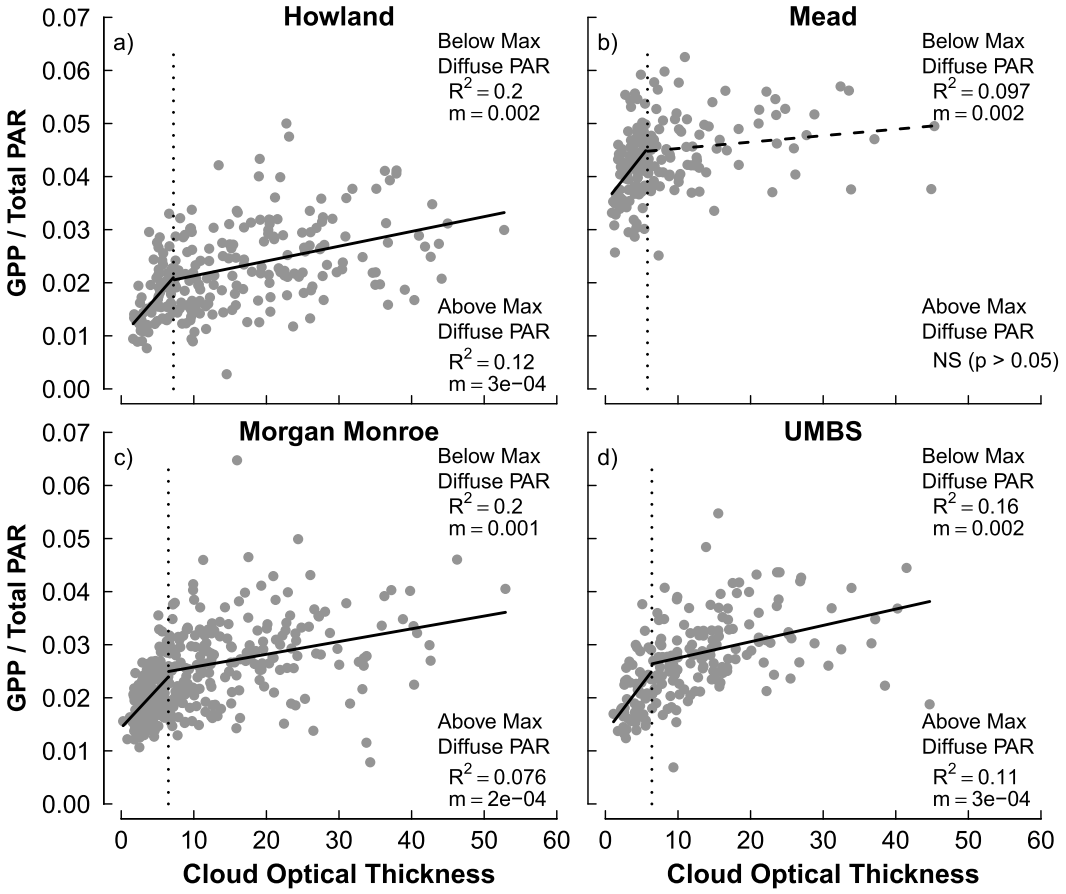

Figure 4. During the peak growing season (average start date and length listed in Table 1), light-use efficiency (gross primary production per unit total PAR) increases with cloud optical thickness (τ_c) at (a) Howland Forest, (b) Mead, (c) Morgan Monroe, and (d) UMBS. The vertical dotted line represents the τ_c where the maximum diffuse PAR occurs at each site (see Figure 1). The peak growing season only covers a portion of time from May through September, which are shown in Figures 1–3. The dashed regression line in Figure 4b indicates a relationship that is not significant (NS; $p > 0.05$). The solid regression lines shown in all panels indicate relationships with $p < 0.01$.

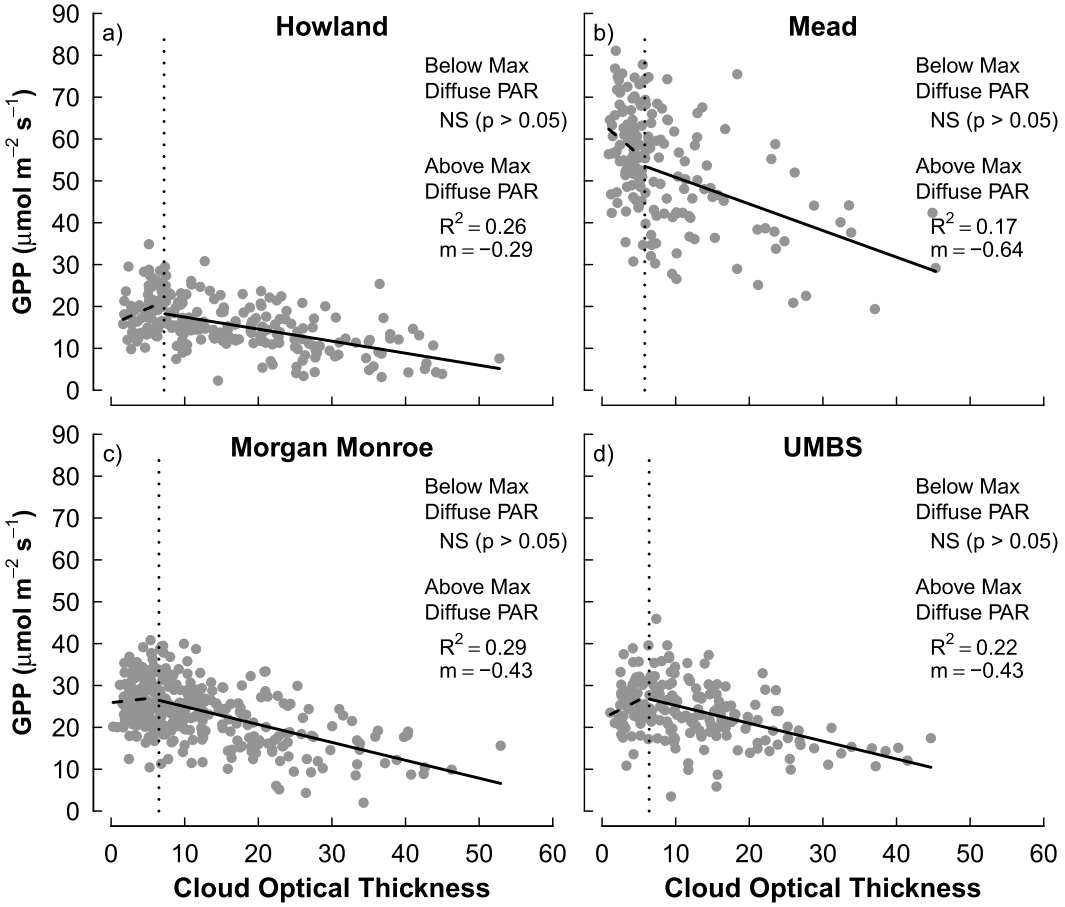

Figure 5. During the peak growing season, there is no significant relationship between cloud optical thickness (τ_c) and gross primary production (GPP) within the site-specific range of τ_c where diffuse photosynthetically active radiation (PAR) increases. The vertical dotted line represents the τ_c for maximum diffuse PAR at each site. The dashed regression lines indicate nonsignificant relationships (NS; $p > 0.05$). The solid regression lines are drawn for relationships with $p < 0.05$.

under optically thin clouds, when diffuse PAR increases with τ_c. Overall, these results suggest that clouds can increase LUE in plant canopies through increases in diffuse PAR.

3.3. τ_c and GPP

Despite the positive relationship between optically thin clouds and LUE, we found no significant relationship between τ_c and canopy GPP at any of the sites while diffuse PAR increases ($p > 0.05$) (Figure 5). This likely occurs because the decrease in total PAR is greater than the increase in diffuse PAR at these sites (Figures 3 and S3). Although sites use light more efficiently under optically thin clouds, the increase in LUE is not large enough to compensate for the decrease in total PAR that occurs under optically thin clouds. In addition, we observed that GPP decreases above the τ_c where the maximum amount of diffuse PAR occurs (Figure 5).

Some studies using diffuse light as a proxy for cloud conditions have concluded that clouds do not increase total canopy productivity [*Alton*, 2008; *Alton et al.*, 2005; *Knohl and Baldocchi*, 2008], while others find support for ecosystem productivity being highest under a moderate amount of cloud cover [*Min and Wang*, 2008; *Rocha et al.*, 2004]. By using satellite-derived τ_c, our results empirically demonstrate that optically thin clouds do not correlate with any net change in ecosystem productivity. The up to 5% decrease in cloud cover observed from satellites during 1984–2007 over the contiguous U.S. [*Sun et al.*, 2015] is, thus, unlikely to have affected the global carbon sink if those changes in cloud cover occurred within a $\tau_c < 7$.

Given the lack of increase between GPP and low τ_c, our study suggests that the diffuse light effect from optically thin clouds may not be a significant driver of GPP at regional or global scales. Importantly, however, one

limitation of our analysis is that we were only able to retrieve τ_c at midday when the effect of diffuse PAR on GPP is smallest in temperate ecosystems [*Cheng et al.*, 2015]. The effect of τ_c on GPP could be stronger at larger zenith angles or in ecosystems located at higher latitudes. However, the larger effect of diffuse light on GPP at larger zenith angles found in *Cheng et al.* [2015] could be independent of cloud conditions, given that diffuse PAR levels are also higher at larger zenith angles [*Earl et al.*, 2012]. In addition, MODIS Collection 5.1 data only retrieve τ_c for pixels assigned as overcast [*Otkin and Greenwald*, 2008]. The response of GPP to clouds could be higher under locally partly cloudy skies (within $3 \times 3\ km^2$) if plants located under clear skies receive diffuse light from nearby clouds [*Law et al.*, 2002]. Overall, our results indicate that the effect of clouds on ecosystem carbon processing through diffuse light is smaller than what was previously concluded from studies that used diffuse light data as a proxy for cloud cover.

4. Conclusions

In this study, we quantify the effect of cloud conditions on surface light and ecosystem GPP and determine the consistency of these relationships across ecosystems with different canopy structures. We evaluate the use of satellite retrievals of globally available τ_c to directly link the effect of clouds to the previously identified positive relationship between diffuse PAR and GPP. Our study expands on previous work by using direct measurements of diffuse PAR and satellite-derived τ_c at several ecosystems instead of using proxies for diffuse light and categories of sky conditions.

We show that only optically thin clouds lead to increases in surface diffuse PAR, while total PAR decreases. In addition, optically thick clouds decrease amounts of both diffuse and total PAR entering plant canopies. Specifically, we define a threshold value of $\tau_c = 6.8$ as the τ_c where diffuse PAR fluxes peak. Moreover, this value is relatively consistent across the ecosystems we studied. Across the range of τ_c where diffuse PAR increases, LUE in forest and maize canopies increases at a higher rate than at larger cloud optical thicknesses when diffuse PAR decreases. However, the increases in LUE under optically thin clouds were too small to compensate for the decreased fluxes of total surface light that occur below the τ_c where diffuse PAR peaks. As a result, low τ_c has no discernable net influence on GPP over the growing season. Despite finding no net effect of optically thin clouds on GPP, our study provides observational evidence for the processes that link atmospheric light conditions to ecosystem carbon uptake. This prompts further examination of how clouds and other drivers of LUE, such as water stress and nutrient availability, interact to alter ecosystem LUE and GPP. For example, if plants are water stressed or nutrient deficient, plants may not be able to take full advantage of the increase in diffuse light that occurs under optically thin clouds.

Overall, satellite measurements and eddy covariance data show that satellite-derived τ_c can be used to estimate the range of cloud conditions that increases surface diffuse light and GPP. Establishing this relationship between diffuse PAR and τ_c allows for predictions of surface diffuse PAR where ground-based measurements are unavailable. In addition, because τ_c accounts for the scattering and absorbing properties of clouds, the use of satellite-derived τ_c allows us to directly link cloud properties to diffuse PAR and GPP. Using these two data sets, our results provide evidence that optically thin clouds do not increase ecosystem GPP. However, optically thick clouds reduce the amount of diffuse and total PAR available for plant canopies and subsequently lead to a decrease in GPP. These results suggest that the diffuse light effect from clouds is not as strong of a driver of regional or global ecosystem productivity in temperate ecosystems during the midday as previously suggested in other studies. We also conclude that there is not a strong relationship between optically thin clouds and climate through diffuse light and the carbon cycle. However, the decreases in diffuse and total light under optically thick clouds could remain an important effect on climate, especially if changes in climate cause clouds to become more optically thick in the future. By empirically linking and quantifying the relationships between τ_c, diffuse PAR, and GPP, we provide insight into how changes in atmospheric conditions alter radiation regimes for terrestrial ecosystems to use for carbon uptake.

Acknowledgments

We acknowledge and thank the following AmeriFlux sites for their data records: US-Ho1, US-Ne1, US-MMS, US-UMB, US-Bar, US-Fuf, US-Snd, and US-Var. We also thank Dori Mermelstein and Stacey Kawecki for their help with NCL scripts, the University of Michigan Center for Statistical Consulting and Research for statistical advisement, and Paul Hubanks and Gala Wind for responding to questions about MODIS data. We also appreciate the thoughtful comments from two anonymous reviewers, Bill Currie, Peter Curtis, Deborah Goldberg, and Gretchen Keppel-Aleks that strengthened the quality of this paper. Funding for S.J.C. was provided in part by the University of Michigan Department of Ecology and Evolutionary Biology Brower Fellowship and the Michigan Space Grant Consortium. A.L.S. was supported in part by NSF AGS 1242203. G.B. was funded in part by NSF 1521238. Funding for AmeriFlux data resources and for core site (US-Ho1, US-Ne1, US-UMB, and US-MMS) data was provided by the U.S. Department of Energy's Office of Science. Data from US-Fuf were also funded by grants from the North American Carbon Program/USDA CREES NRI (2004-35111-15057 and 2008-35101-19076) and Science Foundation Arizona (CAA 0-203-08) awarded to T. Kolb at Northern Arizona University. Additional support for US-Ho1 was provided by the USDA Forest Service Northern Research Station. The data we used in this paper can be found through the AmeriFlux Network (http://ameriflux.lbl.gov/) and NASA's Level 1 and Atmosphere Archive and Distribution System (https://ladsweb.nascom.nasa.gov/data/).

References

Alton, P. B. (2008), Reduced carbon sequestration in terrestrial ecosystems under overcast skies compared to clear skies, *Agric. Forest Meteorol.*, *148*(10), 1641–1653, doi:10.1016/j.agrformet.2008.05.014.

Alton, P. B., P. North, J. Kaduk, and S. Los (2005), Radiative transfer modeling of direct and diffuse sunlight in a Siberian pine forest, *J. Geophys. Res.*, *110*, D23209, doi:10.1029/2005JD006060.

Alton, P. B., P. R. North, and S. O. Los (2007), The impact of diffuse sunlight on canopy light-use efficiency, gross photosynthetic product and net ecosystem exchange in three forest biomes, *Global Change Biol.*, *13*(4), 776–787, doi:10.1111/j.1365-2486.2007.01316.x.

Andrews, T., J. Gregory, P. Forster, and M. Webb (2012), Cloud adjustment and its role in CO_2 radiative forcing and climate sensitivity: A review, *Surv. Geophys.*, *33*(3–4), 619–635, doi:10.1007/s10712-011-9152-0.

Arking, A. (1991), The radiative effects of clouds and their impact on climate, *Bull. Am. Meteorol. Soc.*, *72*(6), 795–813, doi:10.1175/1520-0477(1991)072<0795:TREOCA>2.0.CO;2.

Baldocchi, D. D. (2003), Assessing the eddy covariance technique for evaluating carbon dioxide exchange rates of ecosystems: Past, present and future, *Global Change Biol.*, *9*(4), 479–492, doi:10.1046/j.1365-2486.2003.00629.x.

Barker, H. W., G. L. Stephens, and Q. Fu (1999), The sensitivity of domain-averaged solar fluxes to assumptions about cloud geometry, *Q. J. R. Meteorol. Soc.*, *125*(558), 2127–2152, doi:10.1002/qj.49712555810.

Baum, B., and S. Platnick (2006), Introduction to MODIS Cloud Products, in *Earth Science Satellite Remote Sensing*, edited by J. Qu et al., pp. 74–91, Springer, Berlin, doi:10.1007/978-3-540-37293-6_5.

Bird, R. E., and C. Riordan (1986), Simple solar spectral model for direct and diffuse irradiance on horizontal and tilted planes at the Earth's surface for cloudless atmospheres, *J. Climate Appl. Meteorol.*, *25*(1), 87–97, doi:10.1175/1520-0450(1986)025<0087:SSSMFD>2.0.CO;2.

Bony, S., et al. (2015), Clouds, circulation and climate sensitivity, *Nat. Geosci.*, *8*(4), 261–268, doi:10.1038/ngeo2398.

Boucher, O., et al. (2013), Clouds and aerosols, in *Climate Change 2013: The Physical Science Basis. Contribution of Working Group I to the Fifth Assessment Report of the Intergovernmental Panel on Climate Change*, edited by T. F. Stocker et al., Cambridge Univ. Press, Cambridge, U. K., and New York.

Butt, N., M. New, Y. Malhi, A. C. L. da Costa, P. Oliveira, and J. E. Silva-Espejo (2010), Diffuse radiation and cloud fraction relationships in two contrasting Amazonian rainforest sites, *Agric. Forest Meteorol.*, *150*(3), 361–368, doi:10.1016/j.agrformet.2009.12.004.

Cess, R. D., et al. (1995), Absorption of solar radiation by clouds: Observations versus models, *Science*, *267*(5197), 496–499, doi:10.1126/science.267.5197.496.

Cheng, S. J., G. Bohrer, A. L. Steiner, D. Y. Hollinger, A. Suyker, R. P. Phillips, and K. J. Nadelhoffer (2015), Variations in the influence of diffuse light on gross primary productivity in temperate ecosystems, *Agric. Forest Meteorol.*, *201*, 98–110, doi:10.1016/j.agrformet.2014.11.002.

Chou, M.-D., M. J. Suarez, C.-H. Ho, M. M.-H. Yan, and K.-T. Lee (1998), Parameterizations for cloud overlapping and shortwave single-scattering properties for use in general circulation and cloud ensemble models, *J. Clim.*, *11*(2), 202–214, doi:10.1175/1520-0442(1998)011<0202:PFCOAS>2.0.CO;2.

Davin, E. L., and S. I. Seneviratne (2012), Role of land surface processes and diffuse/direct radiation partitioning in simulating the European climate, *Biogeosciences*, *9*(5), 1695–1707, doi:10.5194/bg-9-1695-2012.

Davis, A. B., and A. Marshak (2010), Solar radiation transport in the cloudy atmosphere: A 3D perspective on observations and climate impacts, *Rep. Prog. Phys.*, *73*(2), 026801.

Dengel, S., and J. Grace (2010), Carbon dioxide exchange and canopy conductance of two coniferous forests under various sky conditions, *Oecologia*, *164*(3), 797–808.

Dim, J. R., T. Takamura, I. Okada, T. Y. Nakajima, and H. Takenaka (2007), Influence of inhomogeneous cloud fields on optical properties retrieved from satellite observations, *J. Geophys. Res.*, *112*, D13202, doi:10.1029/2006JD007891.

Dore, S., M. Montes-Helu, S. C. Hart, B. A. Hungate, G. W. Koch, J. B. Moon, A. J. Finkral, and T. E. Kolb (2012), Recovery of ponderosa pine ecosystem carbon and water fluxes from thinning and stand-replacing fire, *Global Change Biol.*, *18*(10), 3171–3185, doi:10.1111/j.1365-2486.2012.02775.x.

Dragoni, D., H. P. Schmid, C. A. Wayson, H. Potter, C. S. B. Grimmond, and J. C. Randolph (2011), Evidence of increased net ecosystem productivity associated with a longer vegetated season in a deciduous forest in south-central Indiana, USA, *Global Change Biol.*, *17*(2), 886–897, doi:10.1111/j.1365-2486.2010.02281.x.

Earl, H., C. J. Bernacchi, and H. Medrano (2012), Crop photosynthesis, in *Terrestrial Photosynthesis in a Changing Environment*, edited by J. Flexas, F. Loreto, and H. Medrano, 510 pp., Cambridge Univ. Press, Cambridge.

Free, M., and B. Sun (2014), Trends in U.S. total cloud cover from a homogeneity-adjusted dataset, *J. Clim.*, *27*(13), 4959–4969, doi:10.1175/JCLI-D-13-00722.1.

Friedlingstein, P., M. Meinshausen, V. K. Arora, C. D. Jones, A. Anav, S. K. Liddicoat, and R. Knutti (2014), Uncertainties in CMIP5 climate projections due to carbon cycle feedbacks, *J. Clim.*, *27*(2), 511–526, doi:10.1175/JCLI-D-12-00579.1.

Garrity, S. R., G. Bohrer, K. D. Maurer, K. L. Mueller, C. S. Vogel, and P. S. Curtis (2011), A comparison of multiple phenology data sources for estimating seasonal transitions in deciduous forest carbon exchange, *Agric. Forest Meteorol.*, *151*(12), 1741–1752, doi:10.1016/j.agrformet.2011.07.008.

Gough, C. M., B. S. Hardiman, L. E. Nave, G. Bohrer, K. D. Maurer, C. S. Vogel, K. J. Nadelhoffer, and P. S. Curtis (2013), Sustained carbon uptake and storage following moderate disturbance in a Great Lakes forest, *Ecol. Appl.*, *23*(5), 1202–1215, doi:10.1890/12-1554.1.

Gu, L., J. D. Fuentes, H. H. Shugart, R. M. Staebler, and T. A. Black (1999), Responses of net ecosystem exchanges of carbon dioxide to changes in cloudiness: Results from two North American deciduous forests, *J. Geophys. Res.*, *104*(D24), 31,421–31,434, doi:10.1029/1999JD901068.

Gu, L., D. Baldocchi, S. B. Verma, T. A. Black, T. Vesala, E. M. Falge, and P. R. Dowty (2002), Advantages of diffuse radiation for terrestrial ecosystem productivity, *J. Geophys. Res.*, *107*(D6), 4050, doi:10.1029/2001JD001242.

Hansen, J. E. (1971), Multiple scattering of polarized light in planetary atmospheres Part ii. Sunlight reflected by terrestrial water clouds, *J. Atmos. Sci.*, *28*(8), 1400–1426, doi:10.1175/1520-0469(1971)028<1400:MSOPLI>2.0.CO;2.

Hollinger, D. Y., F. M. Kelliher, J. N. Byers, J. E. Hunt, T. M. McSeveny, and P. L. Weir (1994), Carbon dioxide exchange between an undisturbed old-growth temperate forest and the atmosphere, *Ecology*, *75*(1), 134–150, doi:10.2307/1939390.

Hollinger, D. Y., et al. (2004), Spatial and temporal variability in forest-atmosphere CO_2 exchange, *Global Change Biol.*, *10*(10), 1689–1706, doi:10.1111/j.1365-2486.2004.00847.x.

Jenkins, J. P., A. D. Richardson, B. H. Braswell, S. V. Ollinger, D. Y. Hollinger, and M. L. Smith (2007), Refining light-use efficiency calculations for a deciduous forest canopy using simultaneous tower-based carbon flux and radiometric measurements, *Agric. Forest Meteorol.*, *143*(1–2), 64–79, doi:10.1016/j.agrformet.2006.11.008.

Kanniah, K. D., J. Beringer, P. North, and L. Hutley (2012), Control of atmospheric particles on diffuse radiation and terrestrial plant productivity: A review, *Prog. Phys. Geogr.*, *36*(2), 209–237, doi:10.1177/0309133311434244.

Kikuchi, N., T. Nakajima, H. Kumagai, H. Kuroiwa, A. Kamei, R. Nakamura, and T. Y. Nakajima (2006), Cloud optical thickness and effective particle radius derived from transmitted solar radiation measurements: Comparison with cloud radar observations, *J. Geophys. Res.*, *111*, D07205, doi:10.1029/2005JD006363.

King, M. D. (1987), Determination of the scaled optical thickness of clouds from reflected solar radiation measurements, *J. Atmos. Sci.*, *44*(13), 1734–1751, doi:10.1175/1520-0469(1987)044<1734:DOTSOT>2.0.CO;2.
King, M. D., et al. (1997), Cloud retrieval algorithms for MODIS: Optical thickness, effective particle radius, and thermodynamic phase, NASA Goddard Space Flight Cent., Greenbelt, Md.
King, M. D., W. P. Menzel, Y. J. Kaufman, D. Tanre, B. C. Gao, S. Platnick, S. A. Ackerman, L. A. Remer, R. Pincus, and P. A. Hubanks (2003), Cloud and aerosol properties, precipitable water, and profiles of temperature and water vapor from MODIS, *IEEE Trans. Geosci. Remote Sens.*, *41*, 442–458.
King, M. D., S. Platnick, W. P. Menzel, S. A. Ackerman, and P. A. Hubanks (2013), Spatial and temporal distribution of clouds observed by MODIS onboard the Terra and Aqua satellites, *IEEE Trans. Geosci. Remote Sens.*, *51*(7), 3826–3852, doi:10.1109/tgrs.2012.2227333.
Knohl, A., and D. D. Baldocchi (2008), Effects of diffuse radiation on canopy gas exchange processes in a forest ecosystem, *J. Geophys. Res.*, *113*, G02023, doi:10.1029/2007JG000663.
Koren, I., L. Oreopoulos, G. Feingold, L. A. Remer, and O. Altaratz (2008), How small is a small cloud?, *Atmos. Chem. Phys.*, *8*(14), 3855–3864, doi:10.5194/acp-8-3855-2008.
Lauer, A., and K. Hamilton (2013), Simulating clouds with global climate models: A comparison of CMIP5 results with CMIP3 and satellite data, *J. Clim.*, *26*(11), 3823–3845, doi:10.1175/JCLI-D-12-00451.1.
Law, B. E., et al. (2002), Environmental controls over carbon dioxide and water vapor exchange of terrestrial vegetation, *Agric. Forest Meteorol.*, *113*(1–4), 97–120, doi:10.1016/S0168-1923(02)00104-1.
Leontyeva, E., and K. Stamnes (1994), Estimations of cloud optical thickness from ground-based measurements of incoming solar radiation in the Arctic, *J. Clim.*, *7*(4), 566–578, doi:10.1175/1520-0442(1994)007<0566:EOCOTF>2.0.CO;2.
Liu, B. Y. H., and R. C. Jordan (1960), The interrelationship and characteristic distribution of direct, diffuse and total solar radiation, *Solar Energy*, *4*(3), 1–19, doi:10.1016/0038-092X(60)90062-1.
Ma, S., D. D. Baldocchi, J. A. Hatala, M. Detto, and J. Curiel Yuste (2012), Are rain-induced ecosystem respiration pulses enhanced by legacies of antecedent photodegradation in semi-arid environments?, *Agric. Forest Meteorol.*, *154–155*, 203–213, doi:10.1016/j.agrformet.2011.11.007.
Macke, A., P. N. Francis, G. M. McFarquhar, and S. Kinne (1998), The role of ice particle shapes and size distributions in the single scattering properties of cirrus clouds, *J. Atmos. Sci.*, *55*(17), 2874–2883, doi:10.1175/1520-0469(1998)055<2874:TROIPS>2.0.CO;2.
Marchand, R. (2013), Trends in ISCCP, MISR, and MODIS cloud-top-height and optical-depth histograms, *J. Geophys. Res. Atmos.*, *118*, 1941–1949, doi:10.1002/jgrd.50207.
Mayer, B., A. Kylling, S. Madronich, and G. Seckmeyer (1998), Enhanced absorption of UV radiation due to multiple scattering in clouds: Experimental evidence and theoretical explanation, *J. Geophys. Res.*, *103*(D23), 31,241–31,254, doi:10.1029/98JD02676.
Medlyn, B. E. (1998), Physiological basis of the light use efficiency model, *Tree Physiol.*, *18*(3), 167–176.
Mercado, L. M., N. Bellouin, S. Sitch, O. Boucher, C. Huntingford, M. Wild, and P. M. Cox (2009), Impact of changes in diffuse radiation on the global land carbon sink, *Nature*, *458*(7241), 1014–1017, doi:10.1038/nature07949.
Michalsky, J. J., R. Perez, R. Stewart, B. A. LeBaron, and L. Harrison (1988), Design and development of a rotating shadowband radiometer solar radiation/daylight network, *Solar Energy*, *41*(6), 577–581, doi:10.1016/0038-092X(88)90060-6.
Miller, G. R., D. D. Baldocchi, B. E. Law, and T. Meyers (2007), An analysis of soil moisture dynamics using multi-year data from a network of micrometeorological observation sites, *Adv. Water Resour.*, *30*(5), 1065–1081, doi:10.1016/j.advwatres.2006.10.002.
Min, Q. (2005), Impacts of aerosols and clouds on forest-atmosphere carbon exchange, *J. Geophys. Res.*, *110*, D06203, doi:10.1029/2004JD004858.
Min, Q., and S. Wang (2008), Clouds modulate terrestrial carbon uptake in a midlatitude hardwood forest, *Geophys. Res. Lett.*, *35*, L02406, doi:10.1029/2007GL032398.
Niyogi, D., et al. (2004), Direct observations of the effects of aerosol loading on net ecosystem CO_2 exchanges over different landscapes, *Geophys. Res. Lett.*, *31*, L20506, doi:10.1029/2004GL020915.
Oliphant, A. J., D. Dragoni, B. Deng, C. S. B. Grimmond, H. P. Schmid, and S. L. Scott (2011), The role of sky conditions on gross primary production in a mixed deciduous forest, *Agric. Forest Meteorol.*, *151*(7), 781–791, doi:10.1016/j.agrformet.2011.01.005.
Otkin, J. A., and T. J. Greenwald (2008), Comparison of WRF model-simulated and MODIS-derived cloud data, *Mon. Weather Rev.*, *136*(6), 1957–1970, doi:10.1175/2007MWR2293.1.
Pincus, R., S. Platnick, S. A. Ackerman, R. S. Hemler, and R. J. Patrick Hofmann (2012), Reconciling simulated and observed views of clouds: MODIS, ISCCP, and the limits of instrument simulators, *J. Clim.*, *25*(13), 4699–4720, doi:10.1175/JCLI-D-11-00267.1.
Platnick, S., M. D. King, S. A. Ackerman, W. P. Menzel, B. A. Baum, J. C. Riedi, and R. A. Frey (2003), The MODIS cloud products: Algorithms and examples from Terra, *IEEE Trans. Geosci. Remote Sens.*, *41*(2), 459–473, doi:10.1109/tgrs.2002.808301.
Qu, J. J. (2006), *Earth Science Satellite Remote Sensing Vol. 2: Data, Computational Processing, and Tools*, Springer, Berlin.
R Core Team (2014), *R: A Language and Environment for Statistical Computing*, R Foundation for Statistical Computing, Vienna, Austria.
Rocha, A. V., H.-B. Su, C. S. Vogel, H. P. Schmid, and P. S. Curtis (2004), Photosynthetic and water use efficiency responses to diffuse radiation by an aspen-dominated northern hardwood forest, *For. Sci.*, *50*(6), 793–801.
Scott, N. A., C. A. Rodrigues, H. Hughes, J. T. Lee, E. A. Davidson, D. B. Dail, P. Malerba, and D. Y. Hollinger (2004), Changes in carbon storage and net carbon exchange one year after an initial **s**helterwood harvest at Howland Forest, ME, *Environ. Manag.*, *33*(1), S9–S22, doi:10.1007/s00267-003-9114-5.
Shonk, J. K. P., R. J. Hogan, J. M. Edwards, and G. G. Mace (2010), Effect of improving representation of horizontal and vertical cloud structure on the Earth's global radiation budget. Part I: Review and parametrization, *Q. J. R. Meteorol. Soc.*, *136*(650), 1191–1204, doi:10.1002/qj.647.
Steiner, A. L., D. Mermelstein, S. J. Cheng, T. E. Twine, and A. Oliphant (2013), Observed impact of atmospheric aerosols on the surface energy budget, *Earth Interact*, *17*, 1–22.
Stephens, G. L. (2005), Cloud feedbacks in the climate system: A critical review, *J. Clim.*, *18*(2), 237–273, doi:10.1175/JCLI-3243.1.
Still, C. J., et al. (2009), Influence of clouds and diffuse radiation on ecosystem-atmosphere CO_2 and $CO^{18}O$ exchanges, *J. Geophys. Res.*, *114*, G01018, doi:10.1029/2007JG000675.
Sun, B., M. Free, H. L. Yoo, M. J. Foster, A. Heidinger, and K.-G. Karlsson (2015), Variability and trends in U.S. cloud cover: ISCCP, PATMOS-x, and CLARA-A1 compared to homogeneity-adjusted weather observations, *J. Clim.*, *28*(11), 4373–4389, doi:10.1175/JCLI-D-14-00805.1.
Suyker, A. E., and S. B. Verma (2008), Interannual water vapor and energy exchange in an irrigated maize-based agroecosystem, *Agric. Forest Meteorol.*, *148*(3), 417–427, doi:10.1016/j.agrformet.2007.10.005.
Turner, D. P., S. Urbanski, D. Bremer, S. C. Wofsy, T. Meyers, S. T. Gower, and M. Gregory (2003), A cross-biome comparison of daily light use efficiency for gross primary production, *Global Change Biol.*, *9*(3), 383–395, doi:10.1046/j.1365-2486.2003.00573.x.

Twomey, S. (1991), Symposium on global climatic effects of aerosols, clouds and radiation, *Atmos. Environ. Part A General Top.*, *25*(11), 2435–2442, doi:10.1016/0960-1686(91)90159-5.

Urban, O., et al. (2007), Ecophysiological controls over the net ecosystem exchange of mountain spruce stand. Comparison of the response in direct vs. diffuse solar radiation, *Global Change Biol.*, *13*(1), 157–168, doi:10.1111/j.1365-2486.2006.01265.x.

Urban, O., et al. (2012), Impact of clear and cloudy sky conditions on the vertical distribution of photosynthetic CO_2 uptake within a spruce canopy, *Funct. Ecol.*, *26*(1), 46–55, doi:10.1111/j.1365-2435.2011.01934.x.

Várnai, T., and A. Marshak (2002), Observations of three-dimensional radiative effects that influence MODIS cloud optical thickness retrievals, *J. Atmos. Sci.*, *59*(9), 1607–1618, doi:10.1175/1520-0469(2002)059<1607:OOTDRE>2.0.CO;2.

Xu, L., and D. D. Baldocchi (2004), Seasonal variation in carbon dioxide exchange over a Mediterranean annual grassland in California, *Agric. Forest Meteorol.*, *123*(1–2), 79–96, doi:10.1016/j.agrformet.2003.10.004.

Zeng, S., C. Cornet, F. Parol, J. Riedi, and F. Thieuleux (2012), A better understanding of cloud optical thickness derived from the passive sensors MODIS/AQUA and POLDER/PARASOL in the A-Train constellation, *Atmos. Chem. Phys.*, *12*(23), 11,245–11,259, doi:10.5194/acp-12-11245-2012.